The *a2* mating-type-locus gene *lga2* of *Ustilago maydis* interferes with mitochondrial dynamics and fusion, partially in dependence on a Dnm1-like fission component

Michael Mahlert[1,*,‡], Christine Vogler[2], Kathrin Stelter[3], Gerd Hause[4] and Christoph W. Basse[1,*,§,¶]

[1]Max-Planck-Institute for Terrestrial Microbiology, Department Organismic Interactions, 35043 Marburg, Germany
[2]Max-Planck-Institute of Immunobiology, 79108 Freiburg i. Br., Germany
[3]Philipps-Universität Marburg, FB Biologie/Parasitologie, 35043 Marburg, Germany
[4]Martin-Luther-University Halle-Wittenberg, Biocenter, 06099 Halle/Saale, Germany

*These authors contributed equally to this work
‡Present address: Bitplane AG, Badenerstrasse 682, CH-8048 Zürich, Switzerland
§Present address: Institute for Applied Biosciences, University of Karlsruhe, 76187 Karlsruhe, Germany
¶Author for correspondence (e-mail: basse@mpi-marburg.mpg.de)

Accepted 6 April 2009
Journal of Cell Science 122, 2402-2412 Published by The Company of Biologists 2009
doi:10.1242/jcs.039354

Summary

The *a2* mating-type-locus gene *lga2* of the basidiomycete *Ustilago maydis* encodes a mitochondrial protein that interferes with mitochondrial morphology and integrity, and that plays a role in uniparental inheritance of mitochondrial DNA. To address the mode of action of Lga2, we investigated its Dnm1 (a dynamin-related protein)-dependent effects. Here, we demonstrate that Dnm1 functions as a mitochondrial fission component in *U. maydis* and mediates Lga2-induced mitochondrial fragmentation. Mitochondrial fusion occurred very inefficiently in matings of *U. maydis* wild-type strains, but was strongly stimulated in the absence of *dnm1* and highest in either wild-type or *Δdnm1* combinations when the *a2* partner was deleted in *lga2*. This indicates that Dnm1 plays a central role in opposing mitochondrial fusion in response to endogenous *lga2* expression and that Lga2 additionally inhibits fusion in a *dnm1*-independent manner. Our results further show that Lga2 does not stimulate increased turnover of the putative fusion protein Fzo1 and causes mitochondrial branching, loss of mitochondrial DNA and fitness reduction independently of *dnm1*. We conclude that Lga2 acts upstream of Dnm1, but controls mitochondrial integrity independently of Dnm1-mediated fission. In addition, we demonstrate a role of *dnm1* in fungal virulence.

Supplementary material available online at
http://jcs.biologists.org/cgi/content/full/122/14/2402/DC1

Key words: *Ustilago maydis*, Mating-type, Mitochondrial fission, Mitochondrial fusion, Dnm1, Sexual development

Introduction

Fungal mating-type loci determine cell-type identity, coordinate the sexual cycle, and, in a number of human and plant pathogens, are additionally associated with the control of morphological changes and virulence (Kronstad and Staben, 1997; Hsueh and Heitman, 2008; Stanton and Hull, 2007). Confronted with the diversity of fungal mating-type loci, the identification of novel gene functions might uncover pathways of cell specialization and control of sexual reproduction. The basidiomycete fungus *Ustilago maydis* belongs to the widespread group of phytopathogenic smut fungi, infects maize and causes extensive host tumour formation, which provide for massive formation of the sexual teliospores (Martínez-Espinoza et al., 2002; Kahmann et al., 2000). Sexual development of *U. maydis* is controlled by the mating-type loci *a* and *b*. The two alleles of the *a* locus, *a1* and *a2*, provide for pheromone/receptor-based recognition between haploid sporidia and fusion to a dikaryotic cell (Bölker et al., 1992; Spellig et al., 1994). The multiallelic *b* locus contains the divergently transcribed *bE* and *bW* genes encoding homeodomain-containing proteins. The combination of different *b* alleles leads to the formation of a bE/bW heterodimer, which is the key player in pathogenic development (Kahmann and Kämper, 2004). The *a2* locus additionally harbours the *lga2* and *rga2* genes, which encode small, hydrophilic, mitochondrial proteins that lack sequence similarities to database entries of non-related species (Urban et al., 1996a; Bortfeld et al., 2004; Schirawski et al., 2005). Expression of these genes is strictly coupled to sexual development: both *lga2* and *rga2* are induced during mating. In addition, *lga2*, being a target of the bE/bW complex, is strongly upregulated after cell fusion (Urban et al., 1996b; Romeis et al., 2000; Brachmann et al., 2001). Analysis of *U. maydis Δmrb1* mutants has provided insight into the Lga2 function. The constitutively expressed *mrb1* gene encodes a mitochondrial protein of the p32 family, members of which primarily reside in mitochondria. Proteins of the p32 family have diverse regulatory functions, which particularly involve associations with nucleic acids; these functions include modulation of pre-mRNA splicing, gene expression or RNA editing in mitochondrial or extramitochondrial locations (Krainer et al., 1991; Jiang et al., 1999; Hayman et al., 2001). *U. maydis Δmrb1* mutants suffer from a severe proliferation defect during host infection and this defect depends on the presence of *lga2* and *rga2*. In this interplay, *lga2* acts as major component that interferes with pathogenic development. In particular, deletion of *lga2* is sufficient to fully restore pathogenicity of *Δmrb1* mutants (Bortfeld et al., 2004). To gain insight into Lga2 activities, the *lga2* gene was conditionally overexpressed in haploid sporidia. This caused extensive fragmentation of mitochondrial networks, accompanied by strongly reduced cell proliferation and selective mitochondrial DNA (mtDNA) loss.

Furthermore, these effects were exacerbated in *U. maydis Δmrb1* mutant strains, reflecting the antagonistic interplay between Mrb1 and Lga2 (Bortfeld et al., 2004). Selective mtDNA loss in response to *lga2* overexpression might be reconciled with its role in uniparental mtDNA inheritance, in which Lga2 mediates the loss of the *a1*-associated mtDNA during pathogenic development (Fedler et al., 2009). Dikaryotic *Δmrb1* mutants might, therefore, suffer from uncontrolled loss of both mtDNA populations, as previously suggested (Bortfeld et al., 2004). In yeast and mammals, mitochondrial dynamics depends on opposing fission and fusion events (Nunnari et al., 1997; Shaw and Nunnari, 2002; Chen and Chan, 2004; Meeusen and Nunnari, 2005; Merz et al., 2007). In *Saccharomyces cerevisiae*, a central component of mitochondrial fission is the dynamin-related GTPase Dnm1 (mammalian orthologue DRP1), which assembles in spots on the mitochondrial surface and is associated with sites of mitochondrial constriction and division. Mitochondria in yeast *dnm1Δ* mutants are characterised by long tubular structures or form interconnected tubular networks owing to biased fusion (Otsuga et al., 1998; Bleazard et al., 1999; Sesaki and Jensen, 1999; Schauss et al., 2006). By contrast, yeast mutants lacking functional Fzo1, an outer-membrane protein and key component of mitochondrial fusion, display fragmented mitochondria and lose mtDNA (Hermann et al., 1998; Rapaport et al., 1998). This raised the possibility that Lga2 perturbs the balance between fusion and fission and thus causes mitochondrial fragmentation and mtDNA loss.

Here, we report an analysis of the effects of Lga2 in dependence on mitochondrial fission, and address the relationship between Lga2 and Mrb1. We demonstrate that the *U. maydis* dynamin-like protein Dnm1 functions as a mitochondrial fission component and plays a major role in mediating mitochondrial dynamics in response to Lga2. Our results reveal differences in the regulation of mitochondrial fusion between *U. maydis* and *S. cerevisiae*, and point out a direct influence of the mating-type loci in controlling this process.

Results

Overexpression of *lga2* interferes with the formation of mitochondrial tubules

The highly punctuate pattern of mitochondrial-matrix-targeted GFP (mtGFP; encoded in plasmid pMB2-2) in response to *lga2* overexpression implied mitochondrial fragmentation (Bortfeld et al., 2004). To substantiate this Lga2 effect, we analysed mitochondrial structures by electron microscopy in a *Δmrb1* mutant strain, which responds more sensitively to Lga2 than does an isogenic wild-type strain. The *U. maydis* MC2Δmrb1 strain is derived from strain FB2Δmrb1, but carries an ectopic copy of *lga2* under the arabinose-inducible *crg1* promoter (supplementary material Table S1) (Bortfeld et al., 2004; Bottin et al., 1996). Electron microscopy revealed highly elongated mitochondrial tubules with lengths up to 5 μm as well as elaborate ring structures under non-inducing conditions in CM (liquid complete medium) (Fig. 1A,B). By contrast, under conditions of *lga2* expression in CM containing arabinose (CM/Ara), the same strain exclusively exhibited multiple, spherical organelles along with dynamic processes (Fig. 1C-E). To exclude that the observed phenotypes resulted from the medium shift, mitochondria were analysed in a corresponding control strain (FB2Δmrb1/pMB2-2) cultivated in CM/Ara medium; here, mitochondrial tubules were detected (Fig. 1F). Evaluation of cell thin sections from strains MC2Δmrb1 and FB2Δmrb1/pMB2-2 grown in CM/Ara indicated an average number of 10.42±4.05 mitochondria (MC2Δmrb1; n=62 cells) and 4.26±1.89 mitochondria (FB2Δmrb1/pMB2-2; n=100 cells) per cell, although the number of fragmented mitochondria might be underestimated owing to a lower probability to hit a spherical mitochondrion. Together, we infer from these results that *lga2* overexpression influences the dynamics of transitions in mitochondrial morphology in favour of spherical organelles.

Identification of the mitochondrial fission component Dnm1 in *U. maydis*

The finding that *lga2* overexpression stimulated mitochondrial fragmentation raised the issue of whether this required Dnm1. We therefore searched the annotated genomic sequence of *U. maydis* for the gene corresponding to *S. cerevisiae DNM1*. The resulting gene (MIPS accession no. um05378) was designated *dnm1*. A BLASTP search of the deduced amino acid sequence indicated highest similarity to the putative Dnm1 sequence of *Cryptococcus neoformans* (NCBI accession no. XP_569513; 64% identity), 50% identity with yeast Dnm1 (NP_013100) and 53% with human DRP1 (NP_036192). Accordingly, the *U. maydis* Dnm1 sequence comprises two large dynamin domains within the N-terminal (positions 29-244) and middle (positions 253-548) portions as well as a dynamin GTPase effector domain (positions 734-825) at the

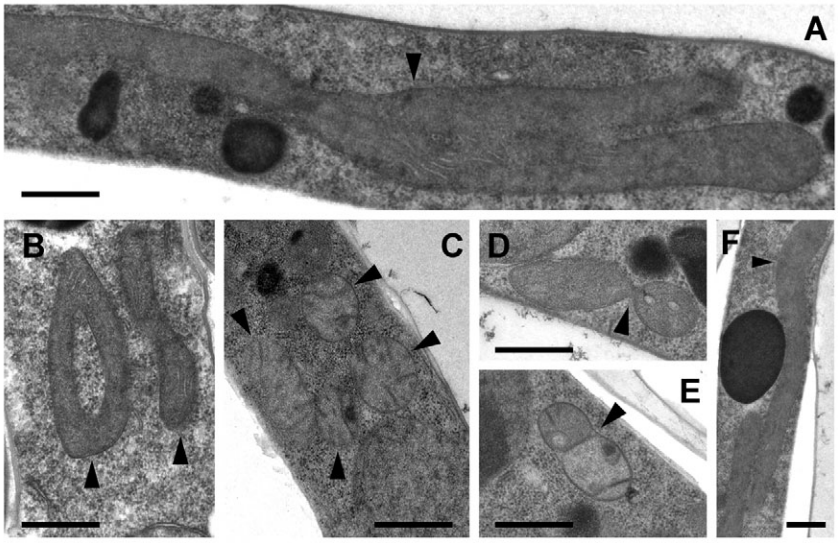

Fig. 1. Mitochondrial morphologies in response to *lga2* overexpression. (A-E) Strain MC2Δmrb1#9 under *lga2*-non-expressing conditions in CM (A,B) and *lga2*-expressing conditions in CM/Ara (C-E). The strain was cultivated in CM, then transferred to either CM (A,B; starting OD_{600}: 0.06) or CM/Ara (C-E; starting OD_{600}: 0.15) for a 13-hour growth period (log-phase). (F) Control strain FB2Δmrb1/pMB2-2 was cultivated in CM/Ara under identical conditions. Arrowheads indicate tubular mitochondrial structures (A,B,F), spherical organelles with cristae (C), a putative constriction site with a measured neck diameter of 75 nm, which fits the expected dimensions of the constriction site (D) (Ingerman et al., 2005), and a mitochondrial pair encapsulated by a continuous membrane resembling mitochondrial fusion intermediates in *S. cerevisiae* cells (E) (Meeusen et al., 2004). Scale bars: 500 nm.

C-terminal portion. The *dnm1* gene was deleted in the *U. maydis* wild-type strain FB2/pKS1, which contains an ectopic insertion of plasmid pKS1 providing for the expression of mtGFP under the *crg1* promoter. Microscopic investigation of sporidia of the resulting *Δdnm1* strain revealed that mitochondria predominantly existed in one or two elongated linear structures frequently spanning the entire cell, whereas two to six smaller fragments were normally detected in wild-type cells (n>40) (supplementary material Fig. S1; see Fig. 2B). Furthermore, *Δdnm1* mitochondria frequently displayed blebs of varying size along a mitochondrial thread (4.1-13.3% of *a1Δdnm1* and *a2Δdnm1* cells, n>200) (see supplementary material Fig. S1; see below). To assure the influence of *dnm1* on mitochondrial morphology, plasmid pCud1, providing for *dnm1* expression under the *crg1* promoter, was introduced into a *Δdnm1* mutant strain constitutively expressing mtGFP. Fluorescence microscopy revealed efficient conversion of extended tubules into smaller fragments under conditions of *dnm1* expression in CM/Ara (Fig. 2A-C), indicating that mitochondrial fragmentation was restored by ectopic expression of *dnm1*.

Next, we investigated the localisation of Dnm1 in *U. maydis*. For this purpose, plasmid pCudg1, encoding an N-terminal fusion of eGFP to Dnm1 expressed from the *crg1* promoter, was ectopically integrated into a haploid strain carrying the reporter construct pKS2, which provides for arabinose-inducible expression of mitochondrial-matrix-targeted red fluorescent protein (mtRFP). Confocal laser microscopy revealed the appearance of Dnm1-GFP in spots (6.6±2.6 spots per cell; n=36 cells), with the majority (89.5%; n=239) being associated with mitochondrial structures (Fig. 2D). The apparent low percentage of Dnm1-GFP spots in the cytosol, their variant sizes and appearance at the side of mitochondria agree with the subcellular distribution and complexity of Dnm1-GFP self-assemblies in yeast (Schauss et al., 2006). To verify mitochondrial localisation, we investigated whether the GFP-fusion derivative cofractionated with mitochondria. This showed that the majority of Dnm1-GFP resided in the mitochondrial fraction 3 hours after inducing its expression in CM/Ara. However, after 6 or 15 hours, the Dnm1-GFP content in the cytosolic fractions was at least as high as in the mitochondrial fractions (Fig. 2E). Furthermore, repeated washing of the mitochondrial pellet in osmotic-stabilising MIB buffer (see Materials and Methods) released Dnm1-GFP protein into the supernatant, suggesting that the protein was not tightly associated with mitochondria (data not shown). This finding is consistent with the localisation of yeast Dnm1 in the cytoplasm and its loose connection to the outer mitochondrial membrane (Otsuga et al., 1998; Schauss et al., 2006).

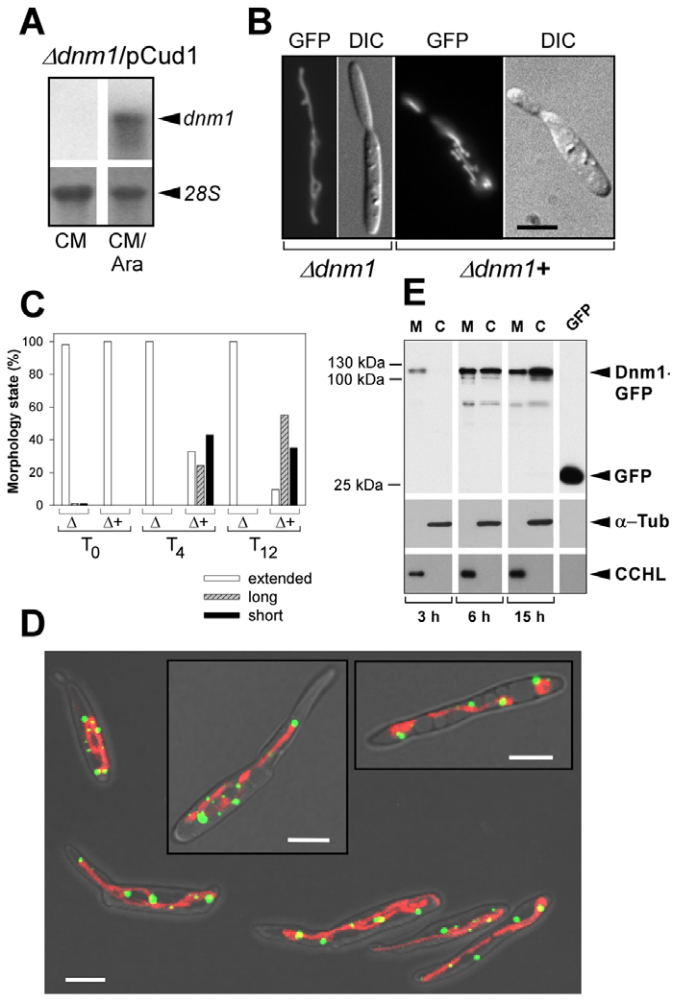

Fig. 2. Mitochondrial morphology of *U. maydis Δdnm1* mutants and localisation of Dnm1-GFP. (A-C) Complementation of the *Δdnm1* phenotype. *Δdnm1* strains were cultivated in CM, then transferred to CM/Ara (starting OD_{600}: 0.35 for A; 0.1 for B,C). (A) Northern blot analysis of *dnm1* transcript levels. RNA was extracted from strain FB1Δdnm1/pMB2-2/pCud1 before (CM) and after 4 hours of growth in CM/Ara. Methylene-blue staining (28S) reflects the amounts of RNA loaded. (B) Comparison of mitochondrial morphologies between strains FB1Δdnm1/pMB2-2 (*Δdnm1*) and FB1Δdnm1/pMB2-2/pCud1 (*Δdnm1*+) after 8 hours in CM/Ara. Representative examples are shown. Scale bar: 5 μm. (C) Quantification of mitochondrial morphology states after induction of *dnm1*. Morphologies were assessed immediately (T_0), 4 hours (T_4) and 12 hours (T_{12}) after transfer to CM/Ara. Extended, continuous fluorescent structures ranging throughout the cell (white bars); long, fluorescent structures spanning >1/3 of the cell length (hatched bars); short, small linear fragments (black bars). n≥100 cells per strain and time point. (D) Confocal microscopy of Dnm1-GFP. Strain BUB7/pKS2/pCudg1 was cultivated in CM, then shifted to CM/Ara for 3 hours (log-phase). Scale bars: 5 μm. (E) Intracellular distribution of Dnm1-GFP. Strain BUB7/pKS2/pCudg1 was cultivated in CM, then shifted to CM/Ara for periods of 3, 6 and 15 hours (starting OD_{600}: 0.35, 0.2 and 0.01, respectively). Proteins from mitochondrial (M; 5 μg) and cytosolic (C; 50 μg) fractions were subjected to SDS-PAGE and immunostained using either anti-GFP, anti-α-tubulin (Tub) or anti-CCHL antibodies. GFP (10 ng) was loaded for size comparison. All lanes for one immunodetection are from the same blot.

Dnm1 and Lga2 interfere with mitochondrial fusion during sexual development

We next addressed whether Dnm1 influenced mitochondrial fusion during sexual development of *U. maydis*. For this purpose, we adopted the mitochondrial fusion assay of yeast (Nunnari et al., 1997). Compatible mating partners carrying the reporter constructs pKS1 or pKS2 (see above) were preloaded with fluorescent proteins in CM/Ara and then shifted to repressing conditions in glucose-containing medium. Dikaryotic hyphae developed 10-12 hours after combining mating partners. The fraction of hyphae attained in these assays was in the range of 5-10% (n>500 cells). In wild-type combinations (FB1 (*a1*)/FB2 (*a2*) and BUB7 (*a1*)/FB2), fusion of mitochondria from opposite mating partners was detected only rarely, even after prolonged incubation for 36 hours (Table 1; data not shown). This inability was not due to a defect in mitochondrial migration in the dikaryon, because mitochondria were able to closely approach each other in most cases (Fig. 3A,B). Strikingly, upon mating of compatible *Δdnm1* strains, fusion of complete mitochondrial structures occurred with frequencies of 57-70%, and

Table 1. Dependence of mitochondrial fusion on *dnm1*, *lga2* and *rga2* in *U. maydis*

Strain combination (*x*/*y*)[a]	State of mitochondrial fusion		
	Fused	Partially fused[b]	Non-fused
	% of hyphae (mean ± s.d.[c])		
FB1/pKS2 × FB2/pKS1 (6/2)	0.9±1.0	0.5±0.8	98.6±1.6
BUB7/pKS2 × FB2/pKS1 (6/2)	2.4±5.1	2.5±3.1	95.1±6.6
FB1Δdnm1/pKS2 × FB2Δdnm1/pKS1 (3/3)	57.2±13.1	3.2±2.2	39.7±13.5
BUB7Δdnm1/pKS2 × FB2Δdnm1/pKS1 (4/2)	70.5±13.0	1.5±1.0	28.1±12.6
FB1/pKS1,2 × FB2Δlga2Δrga2/pKS1,2 (4/3)	91.1±11.5	5.9±6.1	2.9±5.9
BUB7/pKS2 × FB2Δlga2Δrga2/pKS1 (2/2)	83.2	5.5	11.4
FB1/pKS2 × FB2Δlga2/pKS1 (2/2)	92.3	1.9	5.8
BUB7/pKS2 × FB2Δlga2/pKS1 (5/2)	89.3±15.7	3.4±2.5	7.3±14.3
FB1/pKS2 × FB2Δrga2/pKS1 (2/2)	0.0	0.0	100.0
BUB7/pKS2 × FB2Δrga2/pKS1 (1/1)	0.0	1.9	98.1

[a](*x*/*y*): *x*, number of fusion tests performed (each including evaluation of ≥50 hyphae per single test); *y*, number of independent combinations (both mating partners different).
[b]Overlap of GFP and RFP fluorescence in parts of mitochondrial chains (see Fig. 3H).
[c]Standard deviations (s.d.) are indicated in case of ≥ three tests.

thus was strongly increased over mitochondrial fusion in the isogenic wild-type combinations (Table 1; Fig. 3C-E). Taken together, this reinforces a function of Dnm1 as a mitochondrial fission component and implies that Dnm1 opposes mitochondrial fusion in matings between wild-type cells.

Prompted by the strong *lga2* expression in cells harbouring an active b complex (Urban et al., 1996b) and the ability of Lga2 to promote mitochondrial fragmentation, we wondered whether Lga2 interfered with mitochondrial fusion after mating. On the basis of the presumed concerted action of Lga2 and Rga2 (Bortfeld et al., 2004), we first investigated the influence of the *Δlga2Δrga2* double deletion on mitochondrial fusion. Remarkably, in two different strain combinations with the FB2Δlga2Δrga2 partner, fusion of mitochondria from opposite mating partners was detected in 80-90% of dikaryotic hyphae (Table 1). Furthermore, the *lga2* deletion was sufficient to enable mitochondrial fusion with frequencies of ~90%, whereas the *rga2* deletion had no effect (Table 1; Fig. 3F,G). These assays additionally revealed partial mitochondrial fusion events in which only a fraction of parental mitochondrial chains had fused, indicating that mitochondrial fusion was not necessarily completed within the examined period (Fig. 3H; Table 1).

Genetic interaction between *lga2* and *dnm1*

The finding that mitochondrial fusion was strongly stimulated in the absence of either *dnm1* or *lga2* suggested an interplay between the corresponding protein activities. To assess a genetic interaction between *lga2* and *dnm1* with regard to mitochondrial morphology and fusion, plasmid pCLN1, providing for *lga2* overexpression under the *crg1* promoter, was ectopically integrated into the FB2*Δdnm1*/pKS1 strain (*a2*). In the resulting *Δdnm1*/pCLN1 transformants, *lga2* transcript levels were strongly enhanced after transfer to CM/Ara and growth was similarly inhibited as in strain MC2 carrying pCLN1 in a wild-type background (Fig. 4A; see below). Analysis of mitochondrial morphologies in three independent *Δdnm1*/pCLN1 transformants revealed that fragmentation was abolished, whereas *lga2* overexpression in strain MC2 caused extensive fragmentation, as expected (Fig. 4B,C) (Bortfeld et al., 2004). However, the fraction of extended single tubules that is typical for *Δdnm1* cells was markedly reduced in *Δdnm1*/pCLN1 strains, mainly in favour of branched networks (Fig. 4B,C). This indicates that Lga2 requires Dnm1 to cause mitochondrial fragmentation, but exerts an effect on mitochondrial morphology independently of Dnm1.

To assess a *dnm1*-independent effect of Lga2 on mitochondrial fusion, we examined whether conditional *lga2* overexpression compromised fusion in matings between *a1Δdnm1* and *a2Δdnm1*/pCLN1 strains. For this purpose, strains were grown in CM/Ara to express *lga2*, and then shifted to non-inducing CM prior to mating. Complete mitochondrial fusion was detected in 43-77% of dikaryotic cells (Fig. 4D, panel I), and hence was not compromised relative to the *Δdnm1* control combination (Fig. 4D, panels I-III).

To ensure that conditional *lga2* overexpression in the *a2* partner is able to interfere with mitochondrial fusion, *a2Δlga2*/pCLN1 strains were generated. These strains displayed extensive mitochondrial fragmentation when *lga2* was overexpressed in CM/Ara (>97%, *n*>200 cells; data not shown). Mitochondrial fusion was significantly reduced or occurred partially in combinations including these strains, compared with almost complete fusion in combinations with the parental *a2Δlga2* strain (Fig. 4D, panel II). Moreover, mitochondria from the *a2Δlga2*/pCLN1 partner often appeared in smaller fragments in dikaryotic cells (66%, *n*>150), indicative of *lga2* overexpression prior to mating (supplementary material Fig. S2). Taken together, this indicates that conditional overexpression of *lga2* in the *a2Δlga2* partner strongly inhibits mitochondrial fusion, although less efficiently as does endogenous *lga2* expression. This might explain why ectopic *lga2* expression did not impede mitochondrial fusion in *Δdnm1* cells.

To further examine whether *lga2* interferes with mitochondrial fusion independently of *dnm1*, we generated *a2Δlga2Δdnm1* strains. In case of a *dnm1*-independent effect, mitochondrial fusion should be increased in combinations with an *a1Δdnm1* partner relative to the *Δdnm1*/*Δdnm1* combination. Indeed, whereas the *Δdnm1* strain combination gave rise to a mitochondrial fusion frequency of ~50%, as determined from three separate experiments (Fig. 4D, panels I-III), fusion frequencies in combinations including *a2Δlga2Δdnm1* strains were increased and comparable to that obtained in the presence of the *a2Δlga2* partner (Fig. 4D, panel III; see Table 1). This indicates that endogenous *lga2* expression additionally inhibits fusion in a *dnm1*-independent manner.

Overexpression of the *dnm1* genes *drp-1* and *PaDnm1* in *Caenorhabditis elegans* and *Podospora anserina*, respectively, resulted in increased mitochondrial fragmentation (Labrousse et al.,

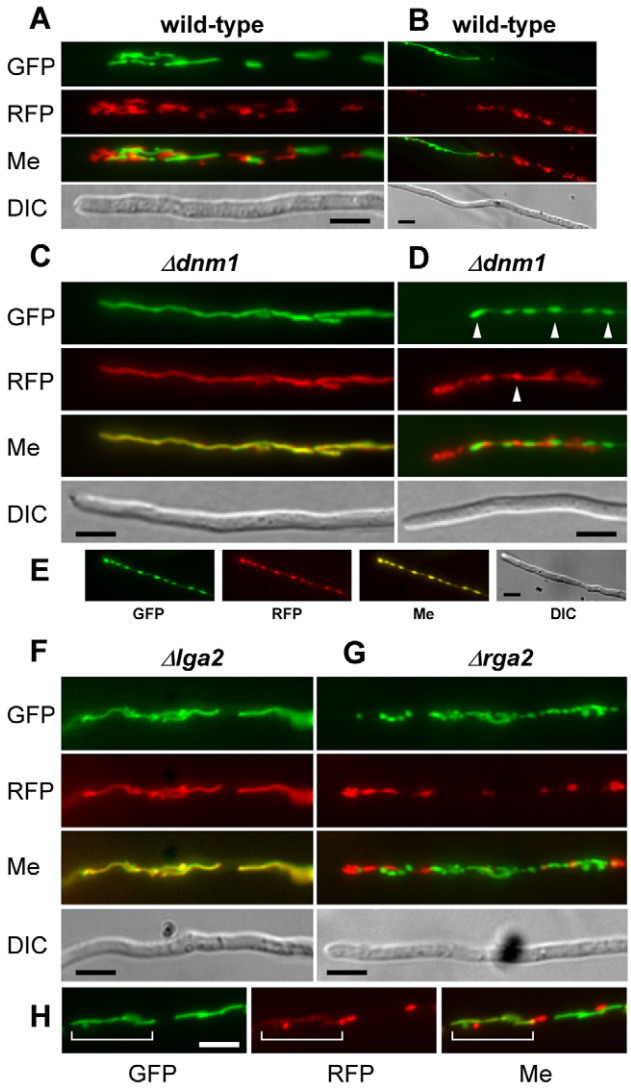

Fig. 3. Investigation of mitochondrial fusion in dependence on *dnm1*, *lga2* and *rga2*. The strain combinations are: (A) FB1/pKS2 × FB2/pKS1. (B) BUB7/pKS2 × FB2/pKS1. (C,D) BUB7Δdnm1/pKS2 × FB2Δdnm1/pKS1. (E) FB1Δdnm1/pKS2 × FB2Δdnm1/pKS1. (F,H) BUB7/pKS2 × FB2Δlga2/pKS1. (G) BUB7/pKS2 × FB2Δrga2/pKS1. (A-G) Mating was performed with cells of opposite mating types preloaded with either mtGFP or mtRFP. Mitochondrial structures in hyphae (DIC) were assayed for GFP and RFP fluorescence 14-18 hours after co-incubation of mating partners. The yellow colour in merged images (Me) indicates coincidence. Representative examples of fused (C,E,F), non-fused (A,B,D,G) and partially fused (H) mitochondria are shown. Note the separation of parental mitochondria in B, mitochondrial blebs in D,E (marked by arrowheads in D), regardless of fusion, and the faint red fluorescence in the region of fusion (bracket) in H. Scale bars: 5 μm.

1999; Scheckhuber et al., 2007). We therefore examined the extent of mitochondrial fragmentation in response to *dnm1* overexpression in *U. maydis* wild-type cells. Northern blot analysis indicated 25- to 30-fold increased *dnm1* transcript levels in FB2/pMB2-2/pCud1 strains under expressing conditions in CM/Ara relative to endogenous transcript levels in the parental strain. Extended overexpression of *dnm1* for 24 hours, however, caused mitochondrial fragmentation in only a minor fraction of cells (<25%) (supplementary material Fig. S3). Together with the finding that *dnm1* transcript levels were not induced in response to *lga2* overexpression (supplementary material Fig. S3), this indicates that Lga2-mediated mitochondrial fragmentation cannot be attributed to transcriptional induction of *dnm1*.

Fzo1 stability in response to Lga2 overexpression

In yeast, the F-box protein Mdm30 regulates the steady-state level of Fzo1, and cells simultaneously overexpressing Mdm30 and Fzo1 have strongly reduced Fzo1 protein levels (Fritz et al., 2003). Prompted by the ability of Lga2 to inhibit mitochondrial fusion, we investigated the levels of the *U. maydis* Fzo1 homologue in response to *lga2* overexpression. The putative *U. maydis* Fzo1 amino acid sequence (957 amino acids; MIPS accession no. um06008) is 29% identical to *S. cerevisiae* Fzo1 (855 amino acids), with highest similarity within the predicted GTPase domain (46% identity). Furthermore, the Fzo1 protein sequence displays a similar arrangement of predicted GTPase, transmembrane and coiled-coil motifs as is found in Fzo1 family proteins (Fig. 5A) (Hales and Fuller, 1997; Hermann et al., 1998). To assess Fzo1 levels in response to *lga2* overexpression, plasmid pCFM1, which, under the *crg1* promoter, expresses full-length Fzo1 C-terminally fused to the Myc epitope, was ectopically integrated into *U. maydis* wild-type and MC2 strains. Under inducing conditions in CM/Ara, *fzo1-myc* transcript levels in FB2/pCFM1 and MC2/pCFM1 strains were similar and exceeded the endogenous *fzo1* levels of the parental strains. Northern blot analysis further confirmed *lga2* overexpression in MC2/pCFM1 strains (Fig. 5B), which, under these conditions, all displayed extensive mitochondrial fragmentation (>80%, n>100). Analysis of Fzo1-Myc protein levels in whole-cell extracts revealed similar signals among independent pCFM1 transformants of strains FB2, MC2#4 and MC2#5 (two of each were analysed) whereas, under repressing conditions in CM, Fzo1-Myc was not detected (data not shown). We next compared steady-state levels of Fzo1-Myc in mitochondrial fractions of FB2/pCFM1 and MC2/pCFM1 strains cultivated in CM/Ara. This revealed similar Fzo1-Myc signals, and no detectable signals in the cytosolic fraction, as expected (Fig. 5C, lanes 9-11; data not shown). Immunoblot analysis further revealed two bands, with the upper one being slightly increased than the expected size of the full-length fusion protein (112 kDa). Currently, we do not have an explanation for the increased mass, but it suggests protein modification. To assess the turnover of Fzo1-Myc in response to *lga2* overexpression, cells were shifted from CM/Ara to non-expressing conditions in CM supplemented with cycloheximide, then Fzo1-Myc levels were determined in mitochondrial fractions during the chase period. Interestingly, this revealed rapid loss of the Fzo1 signal irrespective of preceding *lga2* expression, whereas levels of the intermembrane protein cytochrome C haem lyase (CCHL) (Nicholson et al., 1987), having an apparent molecular mass of 35.8 kDa (MIPS accession no. um01449), were comparable throughout the timecourse (Fig. 5C). Specifically, Fzo1-Myc levels were already halved after a 75-minute chase and reduced by 90-95% after 4 hours. Immunoblot analysis of the cytoplasmic fractions revealed no Myc signals, excluding that the C-terminal Myc signal was cleaved and released to the cytoplasm during the chase (data not shown). In conclusion, Lga2 neither affects the steady-state level of Fzo1 nor promotes Fzo1 turnover.

Analysis of the effects of Lga2 on mitochondrial integrity

Additional effects of *lga2* overexpression are selective mtDNA loss and markedly reduced cell proliferation (Bortfeld et al., 2004). To

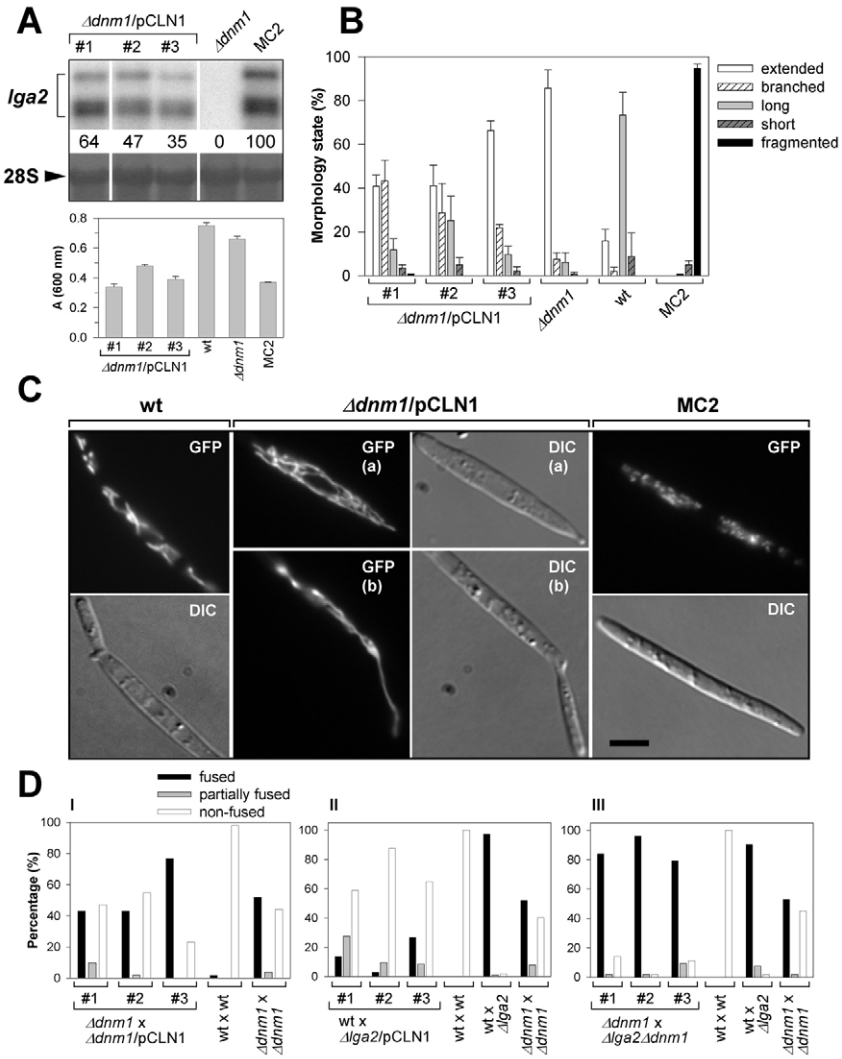

Fig. 4. Genetic interaction between *lga2* and *dnm1*. (A) Northern blot analysis of *lga2* transcript levels in *Δdnm1*/pCLN1 strains, the parental *Δdnm1* strain and MC2 (control). Cells were grown in CM then transferred to CM/Ara for a 12-hour period (log-phase). Both radioactive signals of *lga2* were quantified (value in lane MC2 set to 100). Methylene-blue staining (28S) reflects the amounts of RNA loaded. All lanes are from the same blot. Bottom panel, optical densities of the analysed strains 12 hours after transfer to CM/Ara. Mean values and standard deviations were calculated from cultures in triplicate. (A,B) Strains: FB2Δdnm1/pKS1/pCLN1 (*Δdnm1*/pCLN1; independent transformants #1,2,3), FB2Δdnm1/pKS1 (*Δdnm1*), FB2/pKS1 (wt), MC2#4 (MC2). (B) Quantification of the mitochondrial morphology states after induction of *lga2* in *Δdnm1* strains in log-phase cultures (13-16 hours after transfer to CM/Ara). See Fig. 2C for classification as extended (open bars), long (light grey) and short (hatched dark grey) tubules; fragmented mitochondria (black bars) show a punctuate pattern and the branched phenotype (hatched) shows a ramified network ranging throughout the cell (see C). ≥100 cells were analysed per sample. Mean values and standard deviations were calculated from three experiments. (C) Microscopy of sporidial cells removed from the CM/Ara cultures described in B. Examples of a highly ramified mitochondrial network (a) and an extended tubule (b) in *Δdnm1*/pCLN1 cells. Strain MC2 shows a punctuate mitochondrial pattern compared with linear structures in wild-type cells. Scale bar: 5 μm. (D) Analysis of mitochondrial fusion in dependence on *dnm1* and *lga2*. The strain combinations are: I, FB1Δdnm1/pKS2 × FB2Δdnm1/pKS1/pCLN1; II, FB1/pKS2 × FB2Δlga2/pKS1/pCLN1; III, FB1Δdnm1/pKS2 × FB2Δlga2Δdnm1/pKS1 (#1, #2 and #3 refer to independent transformants of the *a2* partner). The FB1/pKS2 × FB2/pKS1 (wt), FB1Δdnm1/pKS2 × FB2Δdnm1/pKS1 (*Δdnm1*) and FB1/pKS2 × FB2Δlga2/pKS1 (*Δlga2*) combinations served for control. Bars refer to the percentage of fused (black), partially fused (grey) and non-fused (white) mitochondria. ≥50 hyphae were analysed for each strain combination.

assess a causal role of mitochondrial fragmentation, we analysed these effects in MC2Δdnm1 strains in which mitochondrial fragmentation in response to *lga2* overexpression is suppressed (<1.5% fragmentation after a 13-hour growth period in CM/Ara, *n*>150 cells/strain analysed; Fig. 6A). Proliferation rates of MC2 and MC2Δdnm1 strains were, however, similarly reduced and mtDNA loss was not prevented in MC2Δdnm1 strains overexpressing *lga2*, as judged from the decreased ratio of mtDNA:genomic-DNA signals, whereas this ratio remained unchanged in the control strain (Fig. 6B,C). This indicates that mtDNA loss after *lga2* overexpression did not result from mitochondrial fragmentation. Under repressing conditions in CM, neither the growth reduction nor mtDNA loss was seen in MC2Δdnm1 strains (Fig. 6B,C), excluding the possibility that the *Δdnm1* mutation was responsible for these effects.

U. maydis Δmrb1 mutants suffer from a severe proliferation defect during host infection owing to endogenous *lga2* expression and display increased mitochondrial fragmentation in infected tissue. To assess whether the virulence defect of *Δmrb1* mutants results from mitochondrial fragmentation, we generated mating-compatible *Δmrb1Δdnm1* strains. Strains carrying the *Δdnm1* single deletion were included to examine a requirement of *dnm1* for pathogenicity. Combinations of compatible *Δdnm1* or *Δmrb1Δdnm1* strains were not impaired in their ability to mate, as judged from the development of dikaryotic hyphae on solid charcoal medium (data not shown). Formation of disease symptoms, however, was clearly reduced in plants infected with either *Δdnm1* combinations or *Δdnm1* combinations additionally lacking *mrb1* in one mating partner, as assessed from the number of total and severe stem-tumour formation (Fig. 6D). The most prominent difference to the wild type was the strong reduction in stunted or dead plants in infections with compatible *Δdnm1* mutant strains. By contrast, combinations of compatible *Δmrb1Δdnm1* strains were non-pathogenic (Fig. 6D), indicating that the *dnm1* deletion did not suppress the virulence defect of *Δmrb1* mutants. Furthermore, mitochondrial fragmentation was only detected in wild-type strains, but no longer in hyphae of *Δdnm1* mutants during growth in planta (data not shown) (Bortfeld et al., 2004), suggesting that endogenous *lga2* expression in *Δmrb1* mutants affects pathogenic growth regardless of mitochondrial fragmentation.

On the basis of the *dnm1*-independent mode of Lga2, we further examined whether endogenous *lga2* expression compromised the virulence of *U. maydis Δdnm1* mutants. Pathogenicity symptoms caused by the *a1Δdnm1*/*a2Δlga2* control combination were similar to the wild-type infection; however, they were markedly reduced when *dnm1* was additionally deleted in the *a2* partner (Fig. 6D).

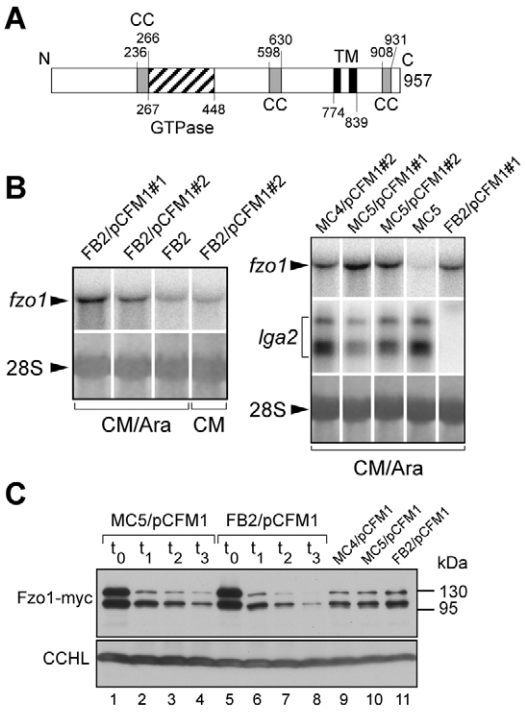

Fig. 5. Fzo1 stability in strains overexpressing *lga2*. (A) Scheme of the predicted domain structure of *U. maydis* Fzo1, showing the positions of the predicted GTPase (hatched), coiled-coil (CC, grey) and transmembrane (TM, closed bar) domains drawn to scale. Amino acid positions are marked. (B) Northern blot analysis of *fzo1* and *lga2* transcript levels in FB2/pCFM1 and MC2/pCFM1 strains (#1 and #2 refer to independent transformants) in comparison with parental strains. RNA was prepared from log-phase cultures in CM/Ara or CM. Methylene blue staining (28S) reflects the amounts of RNA loaded. (C) Steady-state levels and turnover of Fzo1-Myc. Strains were grown in CM, then transferred to CM/Ara (starting OD_{600}: 0.06 for FB2/pCFM1 and 0.12 for MC4,5/pCFM1; transformant #2 was used) for a 14-hour period (log-phase). For the chase, cells were washed in water and transferred to glucose-containing CM containing 100 μg/ml cycloheximide (starting OD_{600}: 0.6). Cells were harvested prior to the chase (t_0) or during the chase at 75 (t_1), 150 (t_2) and 240 (t_3) minutes. Proteins from mitochondrial fractions (30 μg for lanes 1-8 and 10 μg for lanes 9-11) were subjected to SDS-PAGE for immunoblot analysis using anti-C-Myc and anti-CCHL antibodies (loading control).

This indicates a role of *dnm1* in fungal virulence regardless of *lga2*, conceivably by the Dnm1 function in the regulation of mitochondrial morphology.

Submitochondrial localisation of Lga2 and Mrb1

Subcellular localisation of Mrb1-GFP has revealed its distribution to mitochondrial structures and, on the basis of immunoblot analysis, Lga2 and Mrb1 cofractionate with mitochondria (Bortfeld et al., 2004). A thread-like mitochondrial pattern also was detected in a strain expressing the complete *lga2* sequence fused to *eGFP* (Fig. 7A). On the basis of the ability of Lga2 to promote mitochondrial fission and owing to the antagonistic interplay between Lga2 and Mrb1, we examined their submitochondrial localisations. To assess surface localisation, mitochondria that were isolated from strains constitutively expressing either the Lga2-GFP or Mrb1-GFP fusions were treated with proteinase K beads. Interestingly, the Lga2 signal was strongly reduced after treatment, whereas the signal of the CCHL protein was maintained, as expected. Furthermore, the Mrb1-GFP signal was not diminished upon treatment with proteinase K beads, indicating that Mrb1 is not exposed to the mitochondrial surface (Fig. 7B). To exclude that the surface accessibility of Lga2 resulted from overexpression under the constitutive *otef* promoter, we replaced the endogenous *lga2* gene by a construct encoding an N-terminal conjugate of the Myc epitope with Lga2. In the generated strain (CV6), Lga2-Myc was specifically expressed in response to mating and detected solely in the mitochondrial pool (Fig. 7C; data not shown). To assess surface localisation of Lga2-Myc, mitochondria were isolated from pheromone-stimulated CV6 cells and treated with non-immobilised proteinase K because this form was expected to be more accessible than the immobilised enzyme. Indeed, the Lga2-Myc signal was eliminated, whereas the CCHL signal was not affected, indicating that the vast majority of Lga2-Myc was accessible to proteinase K (Fig. 7C).

Prompted by the previously shown association of Mrb1 with both mitochondrial and cytosolic pools (Bortfeld et al., 2004) (supplementary material Fig. S4A), we wondered whether mitochondrial localisation of Mrb1 was a prerequisite for pathogenesis in the presence of *lga2*. To address this issue, we generated strains that, in an *a2Δmrb1* background, express N-terminal conjugates of the Myc epitope with either Mrb1 (CV4) or Mrb1ΔN (CV2), with the latter lacking the N-terminal 40 amino acids of the mitochondrial presequence (supplementary material Fig. S4) (Bortfeld et al., 2004). To assess an influence of the Mrb1 localisation on pathogenicity, these strains were combined with the FB1Δmrb1 mating partner. This indicated that the mitochondrial localisation of Mrb1 is necessary for pathogenesis in combinations of *a1* and *a2* strains (supplementary material Fig. S4; see Discussion).

Discussion

In our study, we analysed the effects of Lga2 on mitochondrial dynamics, their relation to mitochondrial integrity and established an influence of the mating-type loci on mitochondrial fusion during sexual development. Investigation of mitochondrial structures by electron microscopy pointed out that tubular organelles were efficiently converted to spherical organelles in response to Lga2. Furthermore, Lga2-induced mitochondrial fragmentation depends on *dnm1*. Several lines of evidence support a function of Dnm1 in mitochondrial fission. First, *U. maydis Δdnm1* mutants displayed continuous elongated structures with little branching, reminiscent of the mitochondrial morphology of *S. cerevisiae* and *Podospora anserina dnm1Δ* mutants. The appearance of mitochondrial blebs of varying size in *U. maydis Δdnm1* strains might have arisen from local expansion owing to a fission defect, as reported for yeast *dnm1Δ* mutants (Bleazard et al., 1999). Second, conditional overexpression of *dnm1* restored the formation of small mitochondrial chains in *Δdnm1* cells and conferred increased mitochondrial fragmentation in wild-type cells, consistent with overexpression of the *dnm1* genes *drp-1* and *PaDnm1* in *C. elegans* and *P. anserina*, respectively (Labrousse et al., 1999; Scheckhuber et al., 2007). Third, the mitochondrial localisation pattern of Dnm1 and its loose association with mitochondria are reminiscent of the subcellular distribution and aggregation of Dnm1 in yeast (Otsuga et al., 1998; Sesaki and Jensen, 1999; Schauss et al., 2006). Finally, mitochondrial fusion during mating is strongly stimulated in *U. maydis Δdnm1* mutants. The *P. anserina PaDnm1* gene has been shown to be upregulated during transition from the juvenile to the senescent state, which correlated with increased mitochondrial fragmentation (Scheckhuber et al., 2007). However, transcript

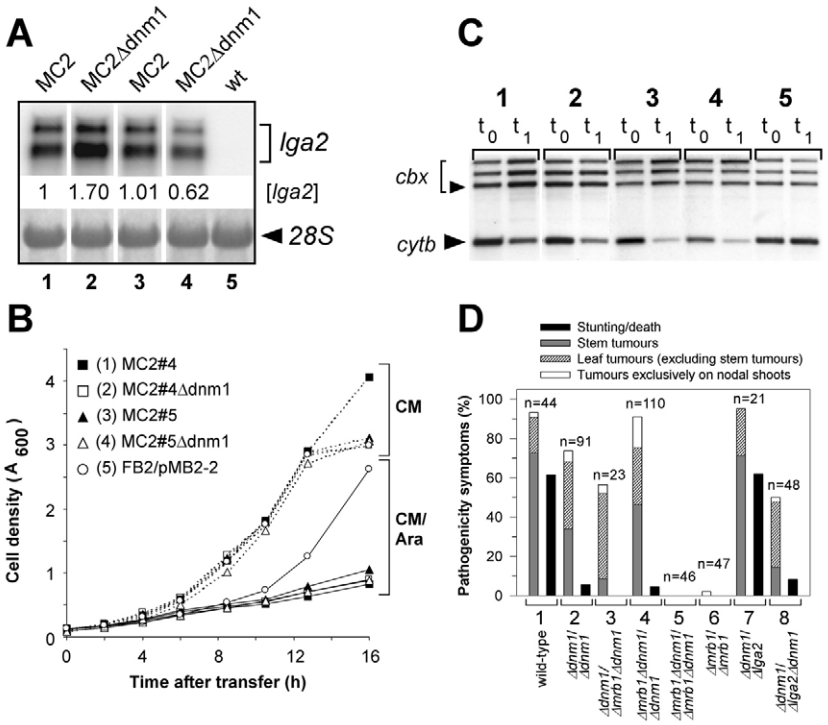

Fig. 6. *dnm1*-independent effects of *lga2*. (A) Northern blot analysis of *lga2* transcript levels in MC2 and MC2Δdnm1 strains 12 hours after shifting to CM/Ara. (1) MC2#4, (2) MC2#4Δdnm1, (3) MC2#5, (4) MC2#5Δdnm1, (5) FB2/pMB2-2 (wt). Both radioactive signals of *lga2* were quantified (value in lane 1 set to 1). Methylene-blue staining (28S) reflects the amounts of RNA loaded. (B) Growth comparison of MC2 and MC2Δdnm1 strains after shifting from CM to either CM/Ara (solid lines) or CM (broken lines). (C) Southern blot analysis comparing the ratios of mtDNA to genomic DNA contents in MC2 and MC2Δdnm1 strains. Strains were cultivated in CM and collected immediately before (t_0) or 12 hours after (t_1) transfer to CM/Ara. Numbers on the top refer to the nomenclature in A. Arrowheads denote the mitochondrial *cytb* and the genomic *cbx* signals. Additional bands stem from plasmid pMB2-2 (*cbx*). All lanes shown are from the same hybridisation. (A-C) Representative examples of each of the two MC2#4Δdnm1 and MC2#5Δdnm1 strains analysed are shown. (D) Pathogenicity test of *U. maydis Δdnm1* and *Δmrb1Δdnm1* mutants. The strain combinations are: (1) FB1/pKS2 × FB2/pKS1, (2) FB1Δdnm1/pKS2 × FB2Δdnm1/pKS1, (3) FB1Δdnm1/pMB2-2 × FB2Δmrb1Δdnm1/pMB2-2, (4) *a1b1*(or *b2*)*Δmrb1Δdnm1* × *a2b2*(or *b1*)*Δdnm1*, (5) *a1b1Δmrb1Δdnm1* × FB2Δmrb1Δdnm1/pMB2-2, (6) *a1b1*(or *b2*)*Δmrb1* × *a2b2*(or *b1*)*Δmrb1*, (7) FB1Δdnm1/pKS2 × FB2Δlga2/pKS1, (8) FB1Δdnm1/pKS2 × FB2Δlga2Δdnm1/pKS1. Strains denoted by their mating types were isolated as meiotic segregants (see Materials and Methods). Plants were inspected 10 or 11 days after inoculation. Stunted plants are characterised by strongly reduced growth and wilting symptoms. *n*, number of inspected plants. For (2), (4), (6) and (8), at least two independent strain combinations were tested. For (1) and (5), each two independent *a1* partners were included.

levels of *dnm1* were not increased by *lga2* overexpression, indicating that endogenous *dnm1* expression is not limiting for Lga2-mediated fragmentation.

In addition, our analysis has demonstrated a role of Lga2 in preventing mitochondrial fusion in dikaryotic cells. This function is fully consistent with strong upregulation of *lga2* in response to an active b complex upon mating (Urban et al., 1996b; Brachmann et al., 2001; Romeis et al., 2000), and emphasizes a connection between the sexual program and the regulation of mitochondrial fusion in *U. maydis*. Significantly, mitochondrial fusion rates were strongly increased in matings of *Δdnm1* strains despite the presence of *lga2*, implying an interplay between Lga2 and Dnm1. Interestingly, fusion rates were highest in *a1*/*a2Δlga2* or *a1Δdnm1*/*a2Δlga2Δdnm1* combinations (see Fig. 4D, panel III), emphasizing that Dnm1 does not oppose mitochondrial fusion in combinations with *Δlga2* strains. Together with the dependency on *dnm1* for mitochondrial fragmentation, we infer from these results that Lga2 acts upstream of Dnm1 to shift the balance towards fission and further prevents fusion independently of Dnm1. Consistent with a *dnm1*-independent effect on mitochondrial morphology, *lga2* overexpression stimulated the formation of branched networks in *Δdnm1* cells (see Fig. 4B,C). Conditional *lga2* overexpression prior to mating impaired mitochondrial fusion less efficiently than endogenous *lga2* expression (see Fig. 4D, panel II). This might be explained by downregulation of *lga2* under the *crg1* promoter in glucose-containing medium during mating, suggesting that the coordination of timing of endogenous *lga2* expression by the b complex is crucial for effective control of fusion.

Crucial steps in mitochondrial division are localisation of Dnm1 at sites of mitochondrial constriction and Dnm1 self-assembly (Bleazard et al., 1999; Shaw and Nunnari, 2002; Ingerman et al., 2005). The finding that Lga2 is exposed to the mitochondrial surface is consistent with a role in promoting fission (Shaw and Nunnari, 2002); however, the underlying mechanism remains to be shown. In contrast to the spot-like appearance of Dnm1, the Lga2-GFP fusion protein displays a thread-like distribution that is maintained in *U. maydis Δdnm1* mutants (see Fig. 7A; data not shown). Furthermore, Lga2 seems to be more tightly associated with mitochondria than Dnm1, because neither Lga2-GFP nor Lga2-Myc are detected in the cytoplasmic portion (Bortfeld et al., 2004) (see Fig. 7C). Together, this argues against a stable Dnm1-Lga2 complex on mitochondria, although we presently cannot exclude a transient interaction under conditions of increased fission.

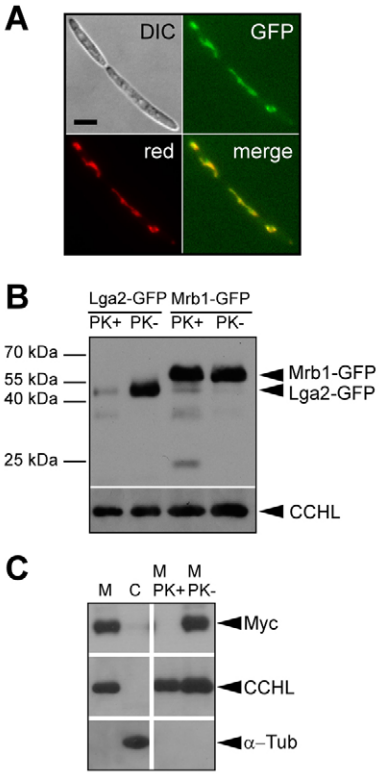

Fig. 7. Submitochondrial localisation of Lga2 and Mrb1. (A) *U. maydis* strain FB2/pLIGC1 (Lga2-GFP) was grown in CM (log-phase), and assayed for GFP fluorescence and the distribution of the marker dye CM-H_2Xros (red). The yellow colour indicates coincidence (merge). Scale bar: 5 µm. (B,C) Sensitivity of Lga2 and Mrb1 to proteinase K treatment. (B) Mitochondria were isolated from strains FB2/pLIGC1 and FB2/pMGH1 (Mrb1-GFP) cultivated in YEPSl. Mitochondria were incubated with proteinase K beads (PK+) or under identical conditions in the absence of beads (PK–). Proteins (2 µg) were subjected to SDS-PAGE for immunoblot analysis. (C) Proteinase K susceptibility of Lga2-Myc expressed under its own regulatory elements in pheromone-treated cells of strain CV6. Mitochondria were either untreated (M), proteinase-K-treated (M PK+) or control-treated (M PK–) in the absence of enzyme. Proteins from mitochondrial (M; 5 µg) and cytosolic (C; 50 µg) fractions were subjected to SDS-PAGE for immunoblot analysis. All lanes for one immunodetection are from the same blot. (B,C) Anti-GFP, anti-CCHL, anti-C-Myc or anti-α-tubulin antibodies were used.

The Lga2 sequence predicts an F-box-like motif, with similarity to that of *S. cerevisiae* Mdm30 (Bortfeld et al., 2004). In *S. cerevisiae*, the two mitochondria-associated F-box proteins Mdm30 and Mbf1 play crucial roles in regulating mitochondrial dynamics (Fritz et al., 2003; Dürr et al., 2006). In particular, Mdm30 plays a main role in regulating the steady-state level of Fzo1 and is required for mitochondrial fusion. Yeast cells simultaneously overexpressing Fzo1 and Mdm30 displayed a high turnover of Fzo1 protein levels compared with a control strain, which expressed normal Mdm30 levels and maintained relatively constant Fzo1 levels over the chase period (Fritz et al., 2003). Interestingly, however, *U. maydis* wild-type cells displayed a high turnover of Fzo1-Myc levels that was not increased in cells simultaneously overexpressing *lga2*. This indicates that Lga2 does not act in the same way as yeast Mdm30, which, in contrast to Lga2, also resides in the cytosol (Fritz et al., 2003).

The low capacity of mitochondrial fusion in *U. maydis* reflects a marked difference to *S. cerevisiae*, in which mitochondrial fusion immediately proceeds with efficiencies of ≥99% in zygotes resulting from the fusion of opposite mating partners (Nunnari et al., 1997; Bleazard et al., 1999). The finding that Lga2 interferes with mitochondrial fusion provides an explanation for this different to behaviour.

In this regard, it will be exciting to explore an influence of the observed high Fzo1 turnover rate on fusion.

Our results have further indicated that the adverse effects of Lga2 on cell proliferation, maintenance of mtDNA and pathogenesis of *U. maydis Δmrb1* mutants do not depend on *dnm1* and hence are not consequences of mitochondrial fission. Lga2-mediated mtDNA loss fully agrees with the recently demonstrated role of Lga2 in uniparental mtDNA inheritance during sexual progression. In particular, Lga2 mediates selective loss of the *a1*-associated mtDNA, and this activity needs to be controlled by Mrb1 to prevent fitness loss. In addition, because genetic exchange between mitochondrial genomes in physically distinct organelles requires mitochondrial fusion (Barr et al., 2005), the ability of Lga2 to interfere with mitochondrial fusion could play a key role in preventing mtDNA exchange, whereas Rga2, which physically interacts with Mrb1, could modulate the effects of Lga2 (Bortfeld et al., 2004; Fedler et al., 2009). Complementation experiments performed in this study have shown that mitochondrial localisation of Mrb1 is essential to restore pathogenicity to *Δmrb1* mutants and thus control the effects of Lga2. Unlike Lga2, Mrb1 is not exposed to the mitochondrial surface, but might reside in the matrix, as suggested from the localisation of the p32 family proteins Mam33p and human p32 (Seytter et al., 1998; Muta et al., 1997). This indicates that the interplay between Lga2 and Mrb1 is indirect and implies that Mrb1 controls the effects of Lga2. It will be challenging to elucidate how Lga2 impacts mitochondria to stimulate fission, whether this activity also mediates selective mtDNA loss and how this is controlled by Mrb1.

Materials and Methods

U. maydis growth conditions

U. maydis growth conditions, mating tests and plant infections were as described previously (Basse et al., 2002; Bortfeld et al., 2004). YEPSl medium contains 1% (w/v) yeast extract, 0.4% (w/v) peptone and 0.4% (w/v) sucrose. CM contains 1% (w/v) glucose and CM/Ara contains 1% (w/v) arabinose instead of glucose. For pheromone stimulation, synthetic Mfa1 pheromone (kindly provided by Michael Feldbrügge, MPI Marburg, Germany) was added to a logarithmically growing culture at a final concentration of 2.5 µg/ml (Koppitz et al., 1996) for 4 hours of incubation in CM.

DNA and RNA procedures

Nucleic-acid procedures and quantification of radioactive signals were performed as described (Basse et al., 2002). *Escherichia coli* K12 strain TOP10 (Invitrogen, Karlsruhe, Germany) was used as a host for cloning. RNA was isolated from liquid cultures using the acidic phenol extraction (Schmitt et al., 1990) (7-12 µg total RNA were loaded per lane). A *Nde*I-*Stu*I *lga2* fragment was isolated from pCLN1 (Bortfeld et al., 2004). A *Bam*HI-*Kpn*I *dnm1* fragment was isolated from plasmid pCud1 (see below). A *fzo1* fragment (positions 1834 to 2874 in the *fzo1* ORF) was amplified from genomic DNA. ^{32}P-labelled *lga2*, *dnm1* and *fzo1* fragments were used for northern blot analysis. Digoxigenin-labelled *cytb* and *cbx* fragments were described (Bortfeld et al., 2004). For PCR, the DNA polymerases Ultra Pfu (Stratagene, Amsterdam, The Netherlands) or Phusion (New England Biolabs, Frankfurt a.M., Germany) were used if not otherwise specified. The correctness of all plasmid constructs was verified by sequencing (ADIS; Max-Planck-Institute, Köln, Germany).

Plasmids and oligonucleotides

Oligonucleotides (see supplementary material Table S2) were synthesised by MWG (Ebersberg, Germany). Plasmids were constructed as described in supplementary material Table S3. The method is discussed in brief below for each plasmid.

pKS1 and pKS2

The *RFP* fragment extended by the *NOST* sequence was isolated from pUMa520 (Becht et al., 2006) as a *Nco*I-*Afl*II fragment to replace the *eGFP-NOST* fragment of

pMB2-2 (Bortfeld et al., 2004). The resulting plasmid and pMB2-2 were used for PCR with primers pril01/02. Products were digested with *Nde*I-*Afl*II and inserted into the respective sites of pRU11 (Brachmann et al., 2001) to yield pKS2 (*mtRFP*) and pKS1 (*mtGFP*).

pCud1

The *dnm1* ORF and 273 bps of 3′-region was inserted into pRU11 replacing the *eGFP-cbx* region as *Nde*I-*Hin*dIII fragment. The nourseothricin (*nat*) resistance cassette isolated as *Not*I fragment from pSL-Nat (A. Brachmann, Die frühe Infektionsphase von *Ustilago maydis*: Genregulation durch das bW/bE-heterodimer, PhD thesis, Max-Planck-Institute for Terrestrial Microbiology, Marburg, 2001) was inserted into the *Not*I site.

pCudg1

The pril05 linker was inserted into pRU11 replacing the *Nde*I-*Hin*dIII fragment to yield pRU11-DL1. The *dnm1* ORF translationally fused to the *eGFP-nat* cassette isolated as a *Sfi*I fragment from pMF5-1n (Becht et al., 2006) was inserted into the *Nco*I-*Sfi*I sites of pRU11-DL1.

pCV11

A 302-bp *NOST Not*I/*Eco*RV fragment of p123 (Aichinger et al., 2003) was introduced into the respective sites 3′ of the *myc* epitope of pEP-DC-tetraCmyc (kindly provided by Jörg Kämper, University of Karlsruhe, Germany).

pCFM1

The *fzo1* ORF linked in frame to the *myc-NOST Sbf*I-*Eco*RV fragment of pCV11 was inserted into pRU11 replacing the *Nde*I-*Hin*dIII fragment. The hygromycin (*hyg*) resistance cassette isolated as a *Not*I(blunt) fragment from pSL-Hyg (A. Brachmann, Die frühe Infektionsphase von *Ustilago maydis*: genregulation durch das bW/bE-heterodimer, PhD thesis, Max-Planck-Institute for Terrestrial Microbiology, Marburg, 2001) was inserted into the *Dra*III(blunt) site.

pCV14

The *mrb1* ORF, deleted for the region encoding amino acids 1-40, extended by 998 bp of 5′ region was generated by PCR-based mutagenesis as described (Farfsing et al., 2005) and inserted into the *Sbf*I site of pCV11 to yield a translational fusion between *mrb1* and *myc*. The 649-bp 3′ region flanking the *mrb1* ORF was introduced into the *Eco*RV-*Nco*I sites 3′ of *NOST*. The *hyg* cassette isolated from pSL-Hyg was inserted into the *Eco*RV site.

pCV16

The 1701-bp *Sbf*I fragment was removed from pCV14 and replaced by a 1821-bp *Sbf*I fragment, amplified from genomic FB2 DNA using primers pril08/11.

pCV25

The *lga2* ORF was translationally fused to the *myc-NOST* of pCV11. Then, the 828-bp *lga2* 3′ region was inserted into the *Eco*RV-*Nco*I sites and the *nat* cassette of pSL-Nat was cloned into the *Eco*RV site.

U. maydis strain construction

All *U. maydis* strains and their genotypes are listed in supplementary material Table S1. Ectopic integration of constructs was verified by diagnostic PCR. *Δdnm1* deletion strains were generated applying a PCR-based protocol (Kämper, 2004). The *dnm1* deletion included positions 1 to 2480 of the 2505-bp *dnm1* ORF. *hyg* or *nat* resistance cassettes were isolated with *Sfi*I from pBShhn and pMF1-n, respectively (Kämper, 2004; Brachmann et al., 2004). For the generation of *a2Δlga2Δdnm1* and *Δmrb1Δdnm1* mutants, the *Δdnm1-nat* construct was transformed into the corresponding *Δlga2* and *Δmrb1* strains, respectively (see supplementary material Table S1). Owing to unsuccessful attempts to obtain homologous recombination in strain FB1Δmrb1/pMB2-2, meiotic segregants from the cross of strains FB1Δdnm1/pMB2-2 and FB2Δmrb1Δdnm1/pMB2-2 were isolated and analysed for the *Δmrb1/Δdnm1* deletions by diagnostic PCR. For a corresponding control experiment (*Δmrb1/Δmrb1* in Fig. 6D), sexual progeny from the cross of strains FB1/pMB2-2 and FB2Δmrb1/pMB2-2 was collected and selected on hygromycin-containing medium. The *Δmrb1* deletion was verified by diagnostic PCR.

For ectopic insertion, plasmids pKS1, pKS2 and pCud1 were cut with *Sca*I and pCudg1 with *Pst*I. For the generation of *a2Δdnm1*/pCLN1 and *a2Δlga2*/pCLN1 strains, plasmid pCLN1 (cut with *Sca*I) was ectopically inserted into the FB2Δdnm1/pKS1 and FB2Δlga2/pKS1 strains. Plasmid pCFM1 was cut with *Pml*I for ectopic insertion into *U. maydis* strains FB2, MC2#4 and MC2#5 to yield strains FB2/pCFM1, MC4/pCFM1 and MC5/pCFM1, respectively. Plasmid pCV25 was cut with *Sca*I for homologous integration into *U. maydis* strain FB2Δmrb1 to yield strain CV6. Homologous integration was verified on either side of the integration by diagnostic PCR. Plasmids pCV14 and pCV16 were cut with *Sfo*I for ectopic insertion into strain FB2Δmrb1 to yield strains CV2 and CV4, respectively.

Investigation of mitochondrial fusion

Compatible *U. maydis* pKS1 and pKS2 reporter strains were cultivated by shaking in CM/Ara (200 rpm; 28°C) for 20-24 hours. Cell pellets were washed in water and resuspended in CM to an OD_{600} of 1.0. After cultivation for an additional 2 hours, collected cell pellets were concentrated in water to an OD_{600} of 3.0. Suspensions of mating partners were mixed (each 0.2 ml) in 2.5 ml screw-cap tubes (Cryo. s; Greiner Bio-One; Frickenhausen, Germany), supplemented with 0.4 ml CM containing 2% (w/v) charcoal (Banuett and Herskowitz, 1994), and incubated on a vertical platform under rotation (10 rpm at 22°C). The air volume was exchanged after 12 hours. For microscopic analysis, cells were immobilised (low-melting agarose; Sigma) and first analysed for RFP fluorescence to avoid photoconversion of GFP.

Protein methods and immunoblot analysis

Mitochondrial and cytosolic protein fractions were prepared from protoplasts in MIB buffer (0.6 M mannitol, 20 mM HEPES-KOH, pH 7.4) containing 1 mM Pefabloc (Roche) as described (Bortfeld et al., 2004). Protein concentrations were determined according to Yaffe (Yaffe, 1991). Mitochondria (50 μg of protein) were incubated in 500 μl MIB buffer supplemented with proteinase K acrylic beads (Sigma; 30 mg/ml equivalent to 0.125 U/ml). The suspension was incubated on a vertical platform under rotation (10 rpm) at 4°C for 2 hours, then centrifuged at 9500 × ***g***. The pellet was resuspended in SDS-containing protein loading buffer, heated (98°C) and beads were removed by centrifugation at 2000 × ***g***. The supernatant was collected, heated again and centrifuged at 16,000 × ***g*** to collect the supernatant. For treatment with non-immobilised proteinase K, mitochondria were incubated in MIB buffer supplemented with 0.4% BSA (w/v) on ice for 30 minutes, then washed in MIB buffer. Mitochondria (~60 μg of protein) in 30 μl MIB buffer were treated with 0.125 U/ml (50 μg/ml) proteinase K (Roche, Mannheim, Germany) for 20 minutes on ice. Reactions were terminated by incubation in the presence of PMSF (0.5 mM) for 10 minutes on ice. Mitochondrial pellets were washed in MIB/PMSF buffer, heated (98°C) in SDS-containing protein loading buffer, and supplemented with PMSF (0.5 mM) prior to freeze storage (–80°C).

Protein amounts as specified in the text were applied to SDS-PAGE (10%) for immunoblot analysis (Basse et al., 2000) using either anti-GFP (Roche), anti-C-Myc (Sigma), anti-α-tubulin (Oncogene Science, Cambridge, MA) or anti-CCHL antibodies (rabbit polyclonal; kind gift of Doron Rapaport, University of Tübingen, Germany). Goat anti mouse IgG-HRP or goat anti rabbit IgG-HRP conjugates (both Promega, Mannheim, Germany) were used as secondary antibodies. Recombinant GFP (10 ng; Roche) was run as control.

Microscopy

Applications of fluorescence microscopy and the mitochondrial marker dye CM-H_2Xros were described (Bortfeld et al., 2004). Confocal images were recorded on a TCS SP5 confocal microscope (Leica, Bensheim, Germany). GFP and RFP fluorescence was monitored applying excitation/emission wavelengths of 488/495-540 nm (GFP) and 568/570-630 nm (RFP). Images were processed by using the imaging software MetaMorph (Universal Imaging, West Chester, PA). For electron microscopy, *U. maydis* strains were cultivated in CM, washed twice in water and transferred to either CM or CM/Ara for 13 hours (log-phase). Electron microscopy was performed as described (Straube et al., 2006).

Databases

Protein sequences were compared with BLASTP of the NCBI database (http://www.ncbi.nlm.nih.gov/). Genomic sequences of *U. maydis* were retrieved from Broad (http://www.broad.mit.edu/annotation/genome/ustilago_maydis/Home.html). Protein sequences and um numbers were retrieved from the MIPS database (http://mips.gsf.de/genre/proj/ustilago/). Prediction of protein motifs was done with PFAM (http://pfam.sanger.ac.uk/search?tab=searchSequenceBlock). Membrane-spanning domains were predicted with TMpred (http://www.expasy.org). Prediction of coiled-coil regions followed the Lupas's method setting the criterion of a probability of >0.4 for at least two windows (http://www.expasy.org).

We thank Kathrin Auffarth for excellent technical assistance, Anna-Lena Müller for support in generating *U. maydis* strains, and Regine Kahmann and Michael Bölker for their comments on the manuscript. We are grateful to Jörg Kämper for kindly providing plasmid pEP-DC-tetraCmyc, to Doron Rapaport for kindly providing the anti-CCHL antibody and to Gunther Doehlemann for assistance with confocal microscopy. In addition, we would like to thank two anonymous reviewers for their suggestions.

References

Aichinger, C., Hansson, K., Eichhorn, H., Lessing, F., Mannhaupt, G., Mewes, W. and Kahmann, R. (2003). Identification of plant-regulated genes in *Ustilago maydis* by enhancer-trapping mutagenesis. *Mol. Genet. Genomics* **270**, 303-314.

Banuett, F. and Herskowitz, I. (1994). Morphological transitions in the life cycle of *Ustilago maydis* and their genetic control by the *a* and *b* loci. *Exp. Mycol.* **18**, 247-266.

Banuett, F. and Herskowitz, I. (1989). Different *a* alleles of *Ustilago maydis* are necessary for maintenance of filamentous growth but not for meiosis. *Proc. Natl. Acad. Sci. USA* **86**, 5878-5882.

Barr, C. M., Neiman, M. and Taylor, D. R. (2005). Inheritance and recombination of mitochondrial genomes in plants, fungi and animals. *New Phytol*. **168**, 39-50.
Basse, C. W., Stumpferl, S. and Kahmann, R. (2000). Characterization of a *Ustilago maydis* gene specifically induced during the biotrophic phase: evidence for negative as well as positive regulation. *Mol. Cell. Biol.* **20**, 321-329.
Basse, C. W., Kolb, S. and Kahmann, R. (2002). A maize-specifically expressed gene cluster in *Ustilago maydis*. *Mol. Microbiol*. **43**, 75-93.
Becht, P., König, J. and Feldbrügge, M. (2006). The RNA-binding protein Rrm4 is essential for polarity in *Ustilago maydis* and shuttles along microtubules. *J. Cell Sci.* **119**, 4964-4973.
Bleazard, W., McCaffery, J. M., King, E. J., Bale, S., Mozdy, A., Tieu, Q., Nunnari, J. and Shaw, J. M. (1999). The dynamin-related GTPase Dnm1 regulates mitochondrial fission in yeast. *Nat. Cell Biol.* **1**, 298-304.
Bölker, M., Urban, M. and Kahmann, R. (1992). The *a* mating type locus of *Ustilago maydis* specifies cell signaling components. *Cell* **68**, 441-450.
Bortfeld, M., Auffarth, K., Kahmann, R. and Basse, C. W. (2004). The *Ustilago maydis a2* mating-type locus genes *lga2* and *rga2* compromise pathogenicity in the absence of the mitochondrial p32 family protein Mrb1. *Plant Cell* **16**, 2233-2248.
Bottin, A., Kämper, J. and Kahmann, R. (1996). Isolation of a carbon source-regulated gene from *Ustilago maydis*. *Mol. Gen. Genet.* **253**, 342-352.
Brachmann, A., Weinzierl, G., Kämper, J. and Kahmann, R. (2001). Identification of genes in the bW/bE regulatory cascade in *Ustilago maydis*. *Mol. Microbiol.* **42**, 1047-1063.
Brachmann, A., König, J., Julius, C. and Feldbrügge, M. (2004). A reverse genetic approach for generating gene replacement mutants in *Ustilago maydis*. *Mol. Genet. Genomics* **272**, 216-226.
Chen, H. and Chan, D. C. (2004). Mitochondrial dynamics in mammals. *Curr. Top. Dev. Biol.* **59**, 119-144.
Dürr, M., Escobar-Henriques, M., Merz, S., Geimer, S., Langer, T. and Westermann, B. (2006). Nonredundant roles of mitochondria-associated F-box proteins Mfb1 and Mdm30 in maintenance of mitochondrial morphology in yeast. *Mol. Biol. Cell* **17**, 3745-3755.
Farfsing, J., Auffarth, K. and Basse, C. W. (2005). Identification of *cis*-active elements in *U. maydis mig2* promoters conferring high-level activity during pathogenic growth in maize. *Mol. Plant Microbe Interact.* **18**, 75-87.
Fedler, M., Luh, K. S., Stelter, K., Nieto, F. and Basse, C. W. (2009). The *a2* mating-type locus genes *lga2* and *rga2* direct uniparental mitochondrial DNA (mtDNA) inheritance and constrain mtDNA recombination during sexual development of *Ustilago maydis*. *Genetics* **181**, 847-860.
Hsueh, Y. P. and Heitman, J. (2008). Orchestration of sexual reproduction and virulence by the fungal mating-type locus. *Curr. Opin. Microbiol.* **11**, 517-524.
Fritz, S., Weinbach, N. and Westermann, B. (2003). Mdm30 is an F-box protein required for maintenance of fusion-competent mitochondria in yeast. *Mol. Biol. Cell* **14**, 2303-2313.
Hales, K. G. and Fuller, M. T. (1997). Developmentally regulated mitochondrial fusion mediated by a conserved, novel, predicted GTPase. *Cell* **90**, 121-129.
Hayman, M. L., Miller, M. M., Chandler, D. M., Goulah, C. C. and Read, L. K. (2001). The trypanosome homolog of human p32 interacts with RBP16 and stimulates its gRNA binding activity. *Nucleic Acids Res.* **29**, 5216-5225.
Hermann, G. J., Thatcher, J. W., Mills, J. P., Hales, K. G., Fuller, M. T., Nunnari, J. and Shaw, J. M. (1998). Mitochondrial fusion in yeast requires the transmembrane GTPase Fzo1p. *J. Cell Biol.* **143**, 359-373.
Ingerman, E., Perkins, E. M., Marino, M., Mears, J. A., McCaffery, J. M., Hinshaw, J. E. and Nunnari, J. (2005). Dnm1 forms spirals that are structurally tailored to fit mitochondria. *J. Cell Biol.* **170**, 1021-1027.
Jiang, J., Zhang, Y., Krainer, A. R. and Xu, R. M. (1999). Crystal structure of human p32, a doughnut-shaped acidic mitochondrial matrix protein. *Proc. Natl. Acad. Sci. USA* **96**, 3572-3577.
Kahmann, R. and Kämper, J. (2004). *Ustilago maydis*: how its biology relates to pathogenic development. *New Phytol.* **164**, 31-42.
Kahmann, R., Steinberg, G., Basse, C., Feldbrügge, M. and Kämper, J. (2000). *Ustilago maydis*, the causative agent of corn smut disease. In *Fungal Pathology* (ed. J. W. Kronstad), pp. 347-371. Kluwer, The Netherlands: Dordrecht.
Kämper, J. (2004). A PCR-based system for highly efficient generation of gene replacement mutants in *Ustilago maydis*. *Mol. Genet. Genomics* **271**, 103-110.
Kämper, J., Kahmann, R., Bölker, M., Ma, L. J., Brefort, T., Saville, B. J., Banuett, F., Kronstad, J. W., Gold, S. E., Müller, O. et al. (2006). Insights form the genome of the biotrophic fungal plant pathogen *Ustilago maydis*. *Nature* **444**, 97-101.
Koppitz, M., Spellig, T., Kahmann, R. and Kessler, H. (1996). Lipoconjugates: structure-activity studies for pheromone analogues of *Ustilago maydis* with varied lipophilicity. *Int. J. Pept. Protein Res.* **48**, 377-390.
Krainer, A. R., Mayeda, A., Kozak, D. and Binns, G. (1991). Functional expression of cloned human splicing factor SF2: homology to RNA-binding proteins, U1 70K, and *Drosophila* splicing regulators. *Cell* **66**, 383-394.
Kronstad, J. W. and Staben, C. (1997). Mating type in filamentous fungi. *Annu. Rev. Genet.* **31**, 245-276.
Labrousse, A. M., Zappaterra, M. D., Rube, D. A. and van der Bliek, A. M. (1999). *C. elegans* dynamin-related protein DRP-1 controls severing of the mitochondrial outer membrane. *Mol. Cell* **4**, 815-826.
Martínez-Espinoza, A. D., Garcia-Pedrajas, M. D. and Gold, S. E. (2002). The Ustilaginales as plant pests and model systems. *Fungal Genet. Biol.* **35**, 1-20.
Meeusen, S., McCaffery, J. M. and Nunnari, J. (2004). Mitochondrial fusion intermediates revealed *in vitro*. *Science* **305**, 1747-1752.
Meeusen, S. L. and Nunnari, J. (2005). How mitochondria fuse. *Curr. Opin. Cell Biol.* **17**, 389-394.
Merz, S., Hammermeister, M., Altmann, K., Dürr, M. and Westermann, B. (2007). Molecular machinery of mitochondrial dynamics in yeast. *Biol. Chem.* **388**, 917-926.
Muta, T., Kang, D., Kitajima, S., Fujiwara, T. and Hamasaki, N. (1997). p32 protein, a splicing factor 2-associated protein, is localized in mitochondrial matrix and is functionally important in maintaining oxidative phosphorylation. *J. Biol. Chem.* **272**, 24363-24370.
Nicholson, D. W., Köhler, H. and Neupert, W. (1987). Import of cytochrome c into mitochondria. Cytochrome c heme lyase. *Eur. J. Biochem.* **164**, 147-157.
Nunnari, J., Marshall, W., Straight, A., Murray, A., Sedat, J. W. and Walter, P. (1997). Mitochondrial transmission during mating in *Saccharomyces cerevisiae* is determined by mitochondrial fusion and fission and the intramitochondrial segregation of mitochondrial DNA. *Mol. Biol. Cell* **8**, 1233-1242.
Otsuga, D., Keegan, B. R., Brisch, E., Thatcher, J. W., Hermann, G. J., Bleazard, W. and Shaw, J. M. (1998). The dynamin-related GTPase, Dnm1p, controls mitochondrial morphology in yeast. *J. Cell Biol.* **143**, 333-349.
Rapaport, D., Brunner, M., Neupert, W. and Westermann, B. (1998). Fzo1p is a mitochondrial outer membrane protein essential for the biogenesis of functional mitochondria in *Saccharomyces cerevisiae*. *J. Biol. Chem.* **273**, 20150-20155.
Romeis, T., Brachmann, A., Kahmann, R. and Kämper, J. (2000). Identification of a target gene for the bE-bW homeodomain protein complex in *Ustilago maydis*. *Mol. Microbiol.* **37**, 54-66.
Schauss, A. C., Bewersdorf, J. and Jakobs, S. (2006). Fis1p and Caf4p, but not Mdv1p, determine the polar localisation of Dnm1p clusters on the mitochondrial surface. *J. Cell Sci*. **119**, 3098-3106.
Scheckhuber, C. Q., Erjavec, N., Tinazli, A., Hamann, A., Nyström, T. and Osiewacz, H. D. (2007). Reducing mitochondrial fission results in increased life span and fitness of two fungal ageing models. *Nat. Cell. Biol.* **9**, 99-105.
Schirawski, J., Heinze, B., Wagenknecht, M. and Kahmann, R. (2005). Mating type loci of *Sporisorium reilianum*: novel pattern with three *a* and multiple *b* specificities. *Eukaryot. Cell* **4**, 1317-1327.
Schmitt, M. E., Brown, T. A. and Trumpower, B. L. (1990). A rapid and simple method for RNA preparation from *Saccharomyces cerevisiae*. *Nucleic Acids Res.* **18**, 3091-3092.
Sesaki, H. and Jensen, R. E. (1999). Division versus fusion: Dnm1p and Fzo1p antagonistically regulate mitochondrial shape. *J. Cell Biol.* **147**, 699-706.
Seytter, T., Lottspeich, F., Neupert, W. and Schwarz, E. (1998). Mam33p, an oligomeric, acidic protein in the mitochondrial matrix of *Saccharomyces cerevisiae* is related to the human complement receptor gC1q-R. *Yeast* **15**, 303-310.
Shaw, J. M. and Nunnari, J. (2002). Mitochondrial dynamics and division in budding yeast. *Trends Cell Biol.* **12**, 178-184.
Spellig, T., Bölker, M., Lottspeich, F., Frank, R. W. and Kahmann, R. (1994). Pheromones trigger filamentous growth in *Ustilago maydis*. *EMBO J.* **13**, 1620-1627.
Stanton, B. C. and Hull, C. M. (2007). Mating-type locus control of cell identity. In *Sex in Fungi: Molecular Determination and Evolutionary Implications* (ed. J. Heitman, J. W. Kronstad, J. W. Taylor and L. A. Casselton), pp. 59-73. Washington, DC: ASM Press.
Straube, A., Hause, G., Fink, G. and Steinberg, G. (2006). Conventional kinesin mediates microtubule-microtubule interactions *in vivo*. *Mol. Biol. Cell* **17**, 907-916.
Urban, M., Kahmann, R. and Bölker, M. (1996a). The biallelic *a* mating type locus of *Ustilago maydis*: remnants of an additional pheromone gene indicate evolution from a multiallelic ancestor. *Mol. Gen. Genet.* **250**, 414-420.
Urban, M., Kahmann, R. and Bölker, M. (1996b). Identification of the pheromone response element in *Ustilago maydis*. *Mol. Gen. Genet.* **251**, 31-37.
Vieira, J. and Messing, J. (1991). New pUC-derived cloning vectors with different selectable markers and DNA replication origins. *Gene* **100**, 189-194.
Yaffe, M. P. (1991). Analysis of mitochondrial function and assembly. *Methods Enzymol.* **194**, 631-634.

Table S1. *U. maydis* strains

Strain	Genotype	Reference
521	*a1 b1*	Kämper et al., 2006
BUB7	*a1 b3*	Basse et al., 2002
FB1	*a1 b1*	Banuett and Herskowitz, 1989
FB2	*a2 b2*	Banuett and Herskowitz, 1989
FB1/pMB2-2	*a1 b1 Potef-mtGFP-cbx^{R}*[a]	Bortfeld et al., 2004
FB2/pMB2-2	*a2 b2 Potef-mtGFP-cbx^{R}*	Bortfeld et al., 2004
FB1_mrb1, FB2_mrb1	*a1 b1 _mrb1::hyg^{R}, a2 b2 _mrb1::hyg^{R}*	Bortfeld et al., 2004
FB1_mrb1/pMB2-2	*a1 b1 _mrb1::hyg^{R} Potef-mtGFP-cbx^{R}*	Bortfeld et al., 2004
FB2_mrb1/pMB2-2	*a2 b2 _mrb1::hyg^{R} Potef-mtGFP-cbx^{R}*	Bortfeld et al., 2004
FB2_lga2	*a2 b2 _lga2::hyg^{R}*	Bortfeld et al., 2004
FB2_rga2	*a2 b2 _rga2::hyg^{R}*	Bortfeld et al., 2004
FB2_lga2_rga2	*a2 b2 _lga2_rga2::hyg^{R}*	Bortfeld et al., 2004
FB2/pLIGC1	*a2 b2 cbx::Potef-lga2-eGFP-cbx^{R}*	Bortfeld et al., 2004
FB2/pMGH1	*a2 b2 mrb1-eGFP-hyg^{R}*	Bortfeld et al., 2004
MC2 (FB2/pMB2-2/pCLN1)	*a2 b2 Potef-mtGFP-cbx^{R} Pcrg1-lga2-nat^{R}*[b]	Bortfeld et al., 2004
MC2_mrb1	*a2 b2 _mrb1::hyg^{R} Potef-mtGFP-cbx^{R} Pcrg1-lga2-nat^{R}*	Bortfeld et al., 2004
MC2_dnm1	*a2 b2 _dnm1::hyg^{R} Potef-mtGFP-cbx^{R} Pcrg1-lga2-nat^{R}*	This study
FB1_dnm1/pMB2-2	*a1 b1 _dnm1::hyg^{R} Potef-mtGFP-cbx^{R}*	This study
FB1_dnm1/pMB2-2/pCud1	*a1 b1 _dnm1::hyg^{R} Potef-mtGFP-cbx^{R} Pcrg1-dnm1-nat^{R}*	This study
FB2/pMB2-2/pCud1	*a2 b2 Potef-mtGFP-cbx^{R} Pcrg1-dnm1-nat^{R}*	This study
FB2_mrb1_dnm1/ pMB2-2	*a2 b2 _mrb1::hyg^{R} _dnm1::nat^{R} Potef-mtGFP-cbx^{R}*	This study
FB1/pKS1, 2	*a1 b1 Pcrg1-mtGFP-cbx^{R}, mtRFP-cbx^{R}*	This study
FB2/pKS1	*a2 b2 Pcrg1-mtGFP-cbx^{R}*	This study
FB1_dnm1/pKS2	*a1 b1 _dnm1::hyg^{R} Pcrg1-mtRFP-cbx^{R}*	This study
FB2_dnm1/pKS1	*a2 b2 _dnm1::hyg^{R} Pcrg1-mtGFP-cbx^{R}*	This study
FB2_dnm1/pKS1/pCLN1	*a2 b2 _dnm1::hyg^{R} Pcrg1-mtGFP-cbx^{R} Pcrg1-lga2-cbx^{R}*	This study
FB2_lga2/pKS1	*a2 b2 _lga2::hyg^{R} Pcrg1-mtGFP-cbx^{R}*	This study
FB2_lga2/pKS1/pCLN1	*a2 b2 _lga2::hyg^{R} Pcrg1-mtGFP-cbx^{R} Pcrg1-lga2-nat^{R}*	This study
FB2_lga2_dnm1/pKS1	*a2 b2 _lga2::hyg^{R} _dnm1::nat^{R} Pcrg1-mtGFP-cbx^{R}*	This study
FB2_rga2/pKS1	*a2 b2 _rga2::hyg^{R} Pcrg1-mtGFP-cbx^{R}*	This study
FB2_lga2_rga2/pKS1, 2	*a2 b2 _lga2_rga2::hyg^{R} Pcrg1-mtGFP-cbx^{R}, mtRFP-cbx^{R}*	This study
BUB7/pKS2	*a1 b3 Pcrg1-mtRFP-cbx^{R}*	This study
BUB7/pKS2/pCudg1	*a1 b3 Pcrg1-mtRFP-cbx^{R} Pcrg1-dnm1-eGFP-nat^{R}*	This study
BUB7_dnm1/pKS2	*a1 b3 _dnm1::hyg^{R} Pcrg1-mtRFP-cbx^{R}*	This study
CV2 (FB2_mrb1/pCV14)	*a2 b2 _mrb1::cbx^{R} mrb1_N-myc-hyg^{R}*	This study
CV4 (FB2_mrb1/pCV16)	*a2 b2 _mrb1::cbx^{R} mrb1-myc-hyg^{R}*	This study
CV6	*a2 b2 _mrb1::cbx^{R} lga2::lga2-myc-nat^{R}*	This study
FB2/pCFM1	*a2 b2 Pcrg1-fzo1-myc-hyg^{R}*	This study
MC2/pCFM1	*a2 b2 Potef-mtGFP-cbx^{R} Pcrg1-lga2-nat^{R} Pcrg1-fzo1-myc-hyg^{R}*	This study

[a] *Potef* : expression under the constitutive *otef* promoter.
[b] *Pcrg1*: expression under the arabinose-inducible *crg1* promoter.

Table S2. Oligonucleotides for plasmid construction

Name	**Sequence** (5' to 3')*	**Use**
pril01	ggaattc**catatg**ATCGCACGCAACTTGTGC	pKS1/2
pril02	CATCGCAAGACCGGCAACAGG	pKS1/2
pril03	aggaattc**attaat**ATGGACGTCGACTTGATTCAGG	pCud1
pril04	ga**aggcct**CCCTTGATCAGCATAAGCACC	pCud1
pril05	**catatg**GCCATGGGCCTGAGTGGCC**aagctt**	pCudg1
pril06	catg**ccatgg**ACGTCGACTTGATTCAGG	pCudg1
pril07	cac**ggccgcgttggcc**GTACTACCACCGCTAGGCTTG	pCudg1
pril08	ttgcaag**cctgcagg**TTGATGAACATGGACGCGAC	pCV14
pril09	GGTAACCGAAAACGTGCGCATTGCTATCGATACACTTCTCAAGATCG	pCV14
pril10	GATCTTGAGAAGTGTATCGATAGCAATGCGCACGTTTTCGGTTACC	pCV14
pril11	agagcgg**cctgcagg**GCATTGATGAAATCGCGCATG	pCV14
pril12	gcag**gatatc**GAATCCGCTCTCGAGCGTTTAGAG	pCV14
pril13	catg**ccatgg**TCTGCGTCGGCCACAACTGCAG	pCV14
pril14	catgatg**cctgcagg**CTATATCCGCCCTTCTCTTCACG	pCV25
pril15	gtaccaa**cctgcagg**GCATCGTCCAGGAAAACGCACATC	pCV25
pril16	ggac**gatatc**ACCCCCTTTGGTATCTGCCCTC	pCV25
pril17	catg**ccatgg**AATCTGGAGAGCAGGCAAACCAAG	pCV25
pril18	ggaattc**catatg**TCCGACAACCACATCG	pCFM1
pril19	cca**atgcat**GCCTTCGAGTCCCTTGAC	pCFM1

*overhangs are in small letters and contained restriction sites are in bold

Table S3. Plasmids

Name	Precursor	Insert, construction	Source/Reference
pUC18	-		Vieira and Messing, 1991
pSL-Nat	-	-	Brachmann, 2001
pSL-Hyg	-	-	Brachmann, 2001
pRU11	-	-	Brachmann et al. 2001
pS	-	-	Basse et al., 2002
p123	-	-	Aichinger et al. 2003
pMB2-2	-	-	Bortfeld et al. 2004
pCLN1	-	-	Bortfeld et al. 2004
pUMa520	-	-	Becht et al., 2006
pMF5-1n	-	-	Becht et al., 2006
pEP-DC-tetraCmyc	pUC18	codon usage-adapted tetra *myc* tag as *Sbf*I/*Not*I fragment	J. Kämper, University of Karlsruhe, Germany
pMBR2	pMB2-2	*mtRFP-NOS* terminator (*NOST*), *Nco*I-*Afl*II *RFP* fragment with *NOST* of pUMa520 cloned into *Nco*I-*Afl*II cut pMB2-2	This study
pKS1	pRU11	*crg1* promoter-*mtGFP-NOST*, *Nde*I/*Afl*II digested PCR (primers: pril01/02, template: pMB2-2) cloned into *Nde*I/*Afl*II cut pRU11	This study
pKS2	pRU11	*crg1* promoter-*mtRFP-NOST*, *Nde*I/*Afl*II digested PCR (primers: pril01/02, template: pMBR2) cloned into *Nde*I/*Afl*II cut pRU11	This study
pCud1v	pRU11	*crg1* promoter-*dnm1* with 273 bp 3'-region, *Ase*I/*Stu*I digested PCR (primers: pril03/04, template: genomic *U. maydis* FB2 DNA) cloned into *Nde*I-*Hind*III(blunt) cut pRU11	This study
pCud1	pCud1v	*nat* cassette, *Not*I *nat* fragment of pSL-Nat cloned into *Not*I cut pCud1v	This study
pRU11-DL1	pRU11	linker, *Nde*I-*Hind*III linker fragment (pril05) cloned into *Nde*I-*Hind*III cut pRU11	This study
pCudg1	pRU11-DL1	*crg1* promoter-*dnm1-eGFP-nat*, *Nco*I/*Sfi*I digested PCR (primers: pril06/07, template: genomic *U. maydis* 521 DNA) linked to *Sfi*I cut *eGFP-nat* of pMF5-1n cloned into *Nco*I/*Sfi*I cut pRU11-DL1	This study
pCV11	pEP-DC-tetraCmyc	*NOST*, *Not*I/*Eco*RV *NOST* fragment of p123 cloned into *Not*I/*Eco*RV cut pEP-DC-tetraCmyc	This study
pCV14vv	pCV11	*mrb1_N* with 998 bp 5'-region, *Sbf*I digested PCR (primer pairs: pril08/09, pril10/11, template: pS) cloned into *Sbf*I cut pCV11	This study
pCV14v	pCV14vv	*mrb1* 649 bp 3'-region, *Eco*RV/*Nco*I digested PCR (primers: pril12/13, template: pS) cloned into *Eco*RV/*Nco*I cut pCV14vv	This study
pCV14	pCV14v	*hyg* cassette, *Not*I(blunt) *hyg* fragment of pSL-Hyg cloned into *Eco*RV cut pCV14v	This study
pCV16	pCV14	*mrb1* with 998 bp 5'-region, 1821 bp *Sbf*I digested PCR (primers: pril08/11, template: pS) replaced 1701 bp *Sbf*I fragment of pCV14	This study
pCV25vv	pCV11	*lga2* fragment, *Sbf*I digested PCR (primers: pril14/15, template: genomic *U. maydis* FB2 DNA) cloned into *Sbf*I cut pCV11	This study
pCV25v	pCV25vv	*lga2* 828 bp 3'-region, *Eco*RV/*Nco*I digested PCR (primers: pril16/17, template: genomic *U. maydis* FB2 DNA) cloned into *Eco*RV/*Nco*I cut pCV25vv	This study
pCV25	pCV25v	*nat* cassette, *Not*I(blunt) *nat* fragment of pSL-Nat	This study

		cloned into *Eco*RV cut pCV25v	
pCFM1v	pRU11	*fzo1*, *Nde*I/*Nsi*I digested PCR (primers: pril18/19, template: genomic *U. maydis* 521 DNA) linked to *Sbf*I/*Eco*RV *myc-NOST* fragment of pCV11 replaced *Nde*I/*Hind*III(blunt) fragment of pRU11	This study
pCFM1	pCFM1v	*hyg* cassette, *Not*I(blunt) *hyg* fragment of pSL-hyg cloned into *Dra*III(blunt) cut pCFM1v	This study